Research, Society and Development, v. 11, n. 6, e22411628770, 2022
(CC BY 4.0) | ISSN 2525-3409 | DOI: http://dx.doi.org/10.33448/rsd-v11i6.28770

Evaluation of three resin cements in the production of cone beam computed tomography artifacts in teeth with fiberglass posts

Avaliação de três cimentos resinosos na produção de artefatos de tomografia computadorizada de feixe cônico em dentes com pinos de fibra de vidro

Evaluación de tres cementos de resina en la producción de artefactos de tomografía computarizada de haz cónico en dientes con postes de fibra de vidrio

Received: 04/02/2022 | Reviewed: 04/09/2022 | Accept: 04/22/2022 | Published: 04/25/2022

Luciana Sarmento de Mendonça
ORCID: https://orcid.org/0000-0001-9468-878X
Universidade de Pernambuco, Brazil
E-mail: lucianasarmento@yahoo.com.br
Laís Maciel Costa
ORCID: https://orcid.org/0000-0003-3880-1914
Universidade de Pernambuco, Brazil
E-mail: laismacielcosta@hotmail.com
José Alcides Almeida de Arruda
ORCID: https://orcid.org/0000-0002-6599-3950
Universidade Federal de Minas Gerais, Brazil
E-mail: alcides_almeida@hotmail.com
Ana Paula Veras Sobral
ORCID: https://orcid.org/0000-0001-6826-0798
Universidade de Pernambuco, Brazil
E-mail: anapvsobral@yahoo.com.br
Maria Luiza dos Anjos Pontual
ORCID: https://orcid.org/0000-0002-5900-8328
Universidade Federal de Pernambuco, Brazil
E-mail: mlpontual@gmail.com
Marcia Maria Fonseca da Silveira
ORCID: https://orcid.org/0000-0002-2611-5661
Universidade de Pernambuco, Brazil
E-mail: marcia.m.f.s@hotmail.com

Abstract

The present study analyzed the presence of artifacts in endodontically treated teeth restored with fiberglass posts (FP) cemented with different resin cements by means of cone beam computed tomography (CBCT) in order to evaluate the contrast-to-noise ratio (CNR). A total of 60 mandibular premolars were selected to assemble the phantoms in order to simulate a clinical situation. The teeth were allocated to 6 groups, in which G1, G2 and G3 were endodontically treated teeth restored with FP cemented with Nexus 3, Duo-Link, and Allcem Core resin cements, respectively; G4: endodontically treated teeth restored with FP; G5: teeth treated only endodontically; and G6: healthy teeth. Mean gray scale values were analyzed in the axial images of the cervical, middle and apical thirds of the post length. CNR analysis was conducted on all groups except G5 and G6. There was a statistically significant difference in the mean values of the middle third region regarding the groups analyzed (p=0.026). However, artifacts were observed in all studied groups. The statistical difference observed between the cervical and apical thirds when the groups were evaluated together did not characterize the absence of artifacts between the resin cements, even when only the FP was present. Consequently, the choice of a resin cement might be based on ease of handling, better working time, cost-effectiveness, activation modes, substrate conditions, and clinical aspects. In summary, image quality was found to be compromised by artifacts in the presence of FP through CBCT with or without the resin cements in the root canal.
Keywords: Artifacts; Cone Beam Computed Tomography; Clinical decision-making; Resin cements.

Resumo

O presente estudo analisou a presença de artefatos em dentes tratados endodonticamente e restaurados com pinos de fibra de vidro (PFV) cimentados com diferentes cimentos resinosos por meio de tomografia computadorizada de feixe cônico (TCFC) para avaliar a relação contraste-ruído (RCR). Um total de 60 pré-molares inferiores foram selecionados para confeccionar os fantomas a fim de simular uma situação clínica. Os dentes foram alocados em 6 grupos, nos quais G1, G2 e G3 foram dentes tratados endodonticamente e restaurados com PFV cimentados com os cimentos resinosos

Nexus 3, Duo-Link e Allcem Core, respectivamente; G4: dentes tratados endodonticamente restaurados com PFV; G5: dentes tratados apenas endodonticamente; e G6: dentes hígidos. Os valores médios da escala de cinza foram analisados nas imagens axiais dos terços cervical, médio e apical do comprimento do pino. A análise da RCR foi realizada em todos os grupos, exceto G5 e G6. Houve diferença estatisticamente significativa nos valores médios da região do terço médio em relação aos grupos analisados (p=0,026). No entanto, artefatos foram observados em todos os grupos estudados. A diferença estatística observada entre os terços cervical e apical quando os grupos foram avaliados em conjunto não caracterizou a ausência de artefatos entre os cimentos resinosos, mesmo quando apenas o PFV estava presente. Consequentemente, a escolha de um cimento resinoso pode ser baseada na facilidade de manuseio, melhor tempo de trabalho, custo-benefício, modos de ativação, condições do substrato e aspectos clínicos. Em resumo, a qualidade da imagem foi comprometida por artefatos na presença de PFV através de TCFC com ou sem os cimentos resinosos no canal radicular.
Palavras-chave: Artefatos; Tomografia Computadorizada de Feixe Cônico; Tomada de decisão clínica; Cimentos de resina.

Resumen
El presente estudio analizó la presencia de artefactos en dientes tratados endodónticamente restaurados con postes de fibra de vidrio (PFV) cementados con cementos de resina diferentes mediante tomografía computarizada de haz cónico (TCHC) para evaluar la relación contraste-ruido (RCR). Se seleccionaron un total de 60 premolares inferiores para realizar los fantomas con el fin de simular una situación clínica. Los dientes fueron asignados en 6 grupos, en los cuales los grupos G1, G2 y G3 fueron dientes tratados endodónticamente, restaurados con PFV y cementados con cementos de resina Nexus 3, Duo-Link y Allcem Core, respectivamente; G4: dientes tratados endodónticamente restaurados con PFV; G5: dientes tratados solo endodónticamente; y G6: dientes sanos. Se analizaron los valores medios de la escala de grises en las imágenes axiales de los tercios cervical, medio y apical de la longitud del poste. El análisis RCR se realizó en todos los grupos excepto G5 y G6. Hubo diferencia estadísticamente significativa en los valores medios de la región del tercio medio en relación a los grupos analizados (p=0,026). Sin embargo, se observaron artefactos en todos los grupos estudiados. La diferencia estadística observada entre los tercios cervical y apical cuando los grupos fueron evaluados juntos no caracterizó la ausencia de artefactos entre los cementos de resina, incluso cuando solo estaba presente el PFV. En consecuencia, la elección de un cemento de resina puede basarse en la facilidad de manejo, mejor tiempo de trabajo, rentabilidad, modos de activación, condiciones del sustrato y aspectos clínicos. En resumen, la calidad de la imagen se vio comprometida por artefactos en presencia de PFV a través de TCHC con o sin cementos de resina en el conducto radicular.
Palabras clave: Artefactos; Tomografía Computarizada de Haz Cónico; Toma de decisiones clínicas; Cementos de resina.

1. Introduction

The loss of tooth structure in endodontically treated teeth is significant and may be associated with the presence of pre-existing dental caries, trauma, and extensive restorations (Carvalho *et al*, 2018). The maintenance of the remaining teeth, especially endodontically treated anterior teeth and premolars, generally requires the use of an intracanal retainer, preferably consisting of fiberglass posts (FP) in oral rehabilitation (Goracci *et al*, 2015). This is mainly due to their dentin-like modulus of elasticity, reduced clinical time and ease of insertion into the tooth (Erik et al., 2019). Various resin cements can be used as bonding agents between FP and the tooth structure. They should have a film thickness that provides adequate marginal sealing and high tensile and compression strength, being radiopaque and esthetic. Furthermore, the maintenance of teeth rehabilitated with an intracanal post has been related to the biological response of the patient (Tanomaru-Filho *et al*, 2008).

It is known that a resin cement with radiopacity distinct from the adjacent dentin promotes better distinction between recurrent caries, empty spaces in the restoration, identification of step, gingival contour, restoration/dental substrate interface, and the presence of an intraradicular retainer such as FP and others not detected in clinicoradiographic evaluations (Altintas *et al*, 2013). In this respect, in order to improve the visualization and distinction between the cements and the remaining tooth structure, high radiopacity values are generally used in dental resin cements (Dukic, 2019). However, when clinical features are not sufficient to establish the diagnosis of an endodontic and/or periodontal lesion, the imaging exams are necessary for decision making both in terms of diagnosis and treatment (Carvalho *et al*, 2021; Celikten *et al*, 2017). Since periapical radiography may occasionally be insufficient to complement the diagnosis, cone beam computed tomography (CBCT) is necessary. The latter is considered to be a very sensitive ancillary diagnostic tool in clinical practice, providing 3D images and thin slices without image overlap which are also particularly useful in the evaluation of root canal systems, cracks/fractures, apical periodontitis, and root resorption (Celikten *et al*, 2017; Petersson *et al*, 2012).

Components with different particles, fillers and radiopacifying agents are added according to the evolution of cementing materials, which aims to advance physical, chemical and biological interactions. Nevertheless, the increase in the radiopacity of the materials does not guarantee a better visualization of the structures in the different image acquisition systems (Bechara *et al*, 2013; Lin *et al*, 2013; Vasconcelos *et al*, 2015). Hence, dental resin cements should be made with radiopacity that facilitates their differentiation between dental tissues, restorative materials and carious lesions, allowing better sharpness and contrast in the visualization of these materials (Altintas *et al*, 2013; Fonseca *et al*, 2006; Rubo & el-Mowafy, 1998; Takeshita *et al*, 2004). In addition, the radiopacity of resin materials is related to the weight content, volume percentage, and chemical composition of the filler particles, particularly radiopaque oxides such as glass, barium, strontium, and zirconia (Toyooka *et al*, 1993; van Dijken; Wing; Ruyter, 1989), which can also be influenced by the thickness of the material (Antonijevic *et al*, 2012; Furtos *et al*, 2012; Pedrosa *et al*, 2011). However, when the composite has excessive radiopacity, the evaluation of filled teeth and dental fissures/fractures can be impaired in the visualization of artifacts thought CBCT images (Draenert *et al*, 2007).

The artifact can be defined as a distortion or error in the reconstructed data that is not present in the investigated object (Schulze *et al*, 2011). For instance, it can appear in different patterns in the form of stripes, line structures and oriented shadows along the projection lines (Vasconcelos *et al*, 2015). On this basis, an objective manner to verify the presence of artifacts is through the analysis of the contrast-to-noise ratio (CNR). This can be estimated on all types of images regardless of compression, scale or output units. The CNR is a measure of lesion detectability since it measures the success rate of an ideal detector in the task of separating healthy and pathological pixels (Rodriguez-Molares *et al*, 2020). Moreover, CNR is a quantitative image quality parameter that has been extensively evaluated in the literature and determined as the ratio between the signal difference (contrast) and the noise level in the image (Yang, 2016). The CNR is also applicable for objective assessment of artifacts. In principle, the greater the number of artifacts, the lower the CNR (Nascimento *et al*, 2019). However, to the best of the authors' knowledge, no study has investigated data on the formation of artifacts in endodontically treated teeth rehabilitated with FP by comparing the CNR among different resin cements. Therefore, the purpose of the present study was to evaluate the presence of artifacts in teeth that received endodontic treatment and FP cemented with three different resin cements using CBCT to measure the CNR.

2. Methodology

2.1 Study design, ethical aspects and sample

The present *in vitro* study complies with the CRIS (Checklist for Reporting In-vitro Studies) guidelines (Krithikadatta; Gopikrishna; Datta, 2014). A total of 60 human premolar teeth extracted for therapeutic reasons were submitted to endodontic treatment, restored or not with FP and resin cements and submitted to the subsequent creation of phantoms. The study was approved by the Ethics Committee of the University of Pernambuco (#057082/2015; #85817317.0.0000.5207).

2.2 Tooth preparation and studied groups

The teeth were disinfected with 0.5% sodium hypochlorite, sterilized in an autoclave and kept in distilled water under refrigeration in order to maintain hydration. The sample (n=10) was allocated to the following groups: G1, G2 and G3 were endodontically treated teeth restored with FP (White Post, FGM, Joinville, SC, Brazil) and cemented with NX3 Nexus™ (Kerr; California, USA), Duo-Link Universal™ (Bisco; Illinois, USA), and Allcem Core (FGM; Joinville, SC, Brazil) resin cements, respectively; G4: endodontically treated teeth restored with FP; G5: teeth treated only endodontically; and G6: healthy teeth.

G5 and G6 were used only in the initial step of the research in order to expose the phantoms to the tomograph, simulating characteristics of a human mouth with the presence of other teeth that could possibly modify image acquisition.

Endodontic treatment of premolars was performed by a single operator (L.S.M.) who had been previously calibrated. The teeth were instrumented up to file #35 (K-File; Dentsply-Ballaigues, Switzerland), 1.0 mm below the apical foramen, using the cervical preparation technique proposed by a previously published method (Estrela *et al*, 1999). The selected teeth were filled with Sealer 26 endodontic cement (Dentsply, Petrópolis, RJ, Brazil) and main and accessories gutta-percha cones (Dentsply-Maillefer, Ballaigues, Switzerland), following the manufacturer's recommendations. After endodontic treatment, the space for the prefabricated post was prepared as described in previous studies (Carvalho *et* al, 2018; Soares *et al*, 2018). Next, their clinical crowns were sectioned with the aid of a micromotor as straight piece and double-faced discs under constant irrigation in order not to heat the dental tissue, 3.0 mm above the cemento-enamel junction. A 4.0 mm obturation remnant was ensured in the apical third of the canal, measured with a precision digital caliper (Digimess 100.174BL; Instrumentos de Precisão Ltda. São Paulo, SP, Brazil).

The FP were selected in thickness according to the diameter of the root canals. From the apical locking of the FP (mechanical action), the resin cements were manipulated according to the manufacturers' instructions and using their own disperser. A thin film of resin cement was inserted into the ducts ensuring uniform thickness. The FP were inserted with enough pressure for the resin cement to flow and light cured (1200 mW/cm2, Radii-cal, SDI, Bayswater, Australia). Excess resin cement was removed and the length of the FP in the coronary portion was compatible with the reconstruction of the coronary core. This was built with direct composite resin (Llis - FGM, Joinville, SC, Brazil) with an average height of 3.0 mm. Excess FP was cut with a diamond tip under irrigation and the composite resin was then finished and polished.

2.3 Phantom preparation

According to the previously published methodology (Carvalho *et al*, 2021), a partially edentulous human mandible belonging to the collection of anatomical pieces of the Oral and Maxillofacial Radiology Department, Federal University of Pernambuco, with its alveoli preserved, was used. Ten healthy teeth which were not part of the study were inserted to compose the dental arch (i.e., central and lateral incisors, canines, and first and second molars of both hemiarches). The premolars (n=60) were previously identified according to each group. The exchange of mandibular premolars was done by drawing lots (https://sorteador.com.br/). Phantoms were identified in order to obtain a template from the acquired images. Tomographic acquisitions were performed using the i-Cat New Generation® Cone Beam Computed Tomograph (Imaging Sciences International, Hatfield, Pennsylvania, USA) with 90 kV, 37.07 mA, FOV of 16 cm, acquisition time of 26.9 seconds, and voxel 0.2 (high resolution protocol) defined in a pilot study.

2.4 CBCT image acquisition

The experimental arrangement was inserted into a polyvinyl chloride (PVC) container with water to simulate the attenuation of the X-ray beam, which occurs due to the presence of soft tissue and generates the scattered retro-radiation (Fagundes *et al*, 2014). The arrangement was positioned on an acrylic platform at the appropriate height using the tomograph light guides so that the images were obtained in the same manner as in the oral cavity. Fifteen tomographic exposures were performed so that all teeth in the study participated randomly (https://sorteador.com.br/). The images saved in XSTD (Xoran) format were exported to the Xoran/Cat® software (Xoran Thechnologies, Ann Arbor, USA), allowing the observation of axial, sagittal and coronal sections and the evaluation of the entire image volume according to the guidelines of the American Association of Endodontics and the American Academy of Oral and Maxillofacial Radiology.

2.5 Image evaluation

An experienced oral and maxillofacial radiologist (M.M.F.S.) selected three axial reconstructions for each premolar, one for each third of the tooth (cervical, middle and apical) and one sagittal reconstruction (Figure 1). Slices were selected at 2.0, 4.0 and 6.0 mm below the cemento-enamel junction (CEJ), representing the cervical, middle and apical region, respectively, of the root third (Freitas *et al*, 2018). These measurements corresponded to the length of the FP and the preparation of the root canal for the intracanal materials (i.e., two thirds of the root). The apical portion of the study teeth was not evaluated (Diniz de Lima *et al*, 2019). After volumetric acquisition, a template was assembled in pdf format for each tooth, containing three axial reconstructions (cervical, middle and apical thirds) and a sagittal section, for objective quantification of artifacts. The selection of slices tends to reduce discrepancies in the location and amount of fill material per area. In total, 60 imaging sections were performed, 4 for each premolar. The thickness of the sections and the distance between them was 1.0 mm, and the filter used was the Sharpen Mild. Each hemiarch was studied in turn.

Figure 1. Axial (cervical, middle and apical) and sagittal sections in template, for evaluation of each tooth exposed to i-Cat New Generation® cone-beam computed tomography.

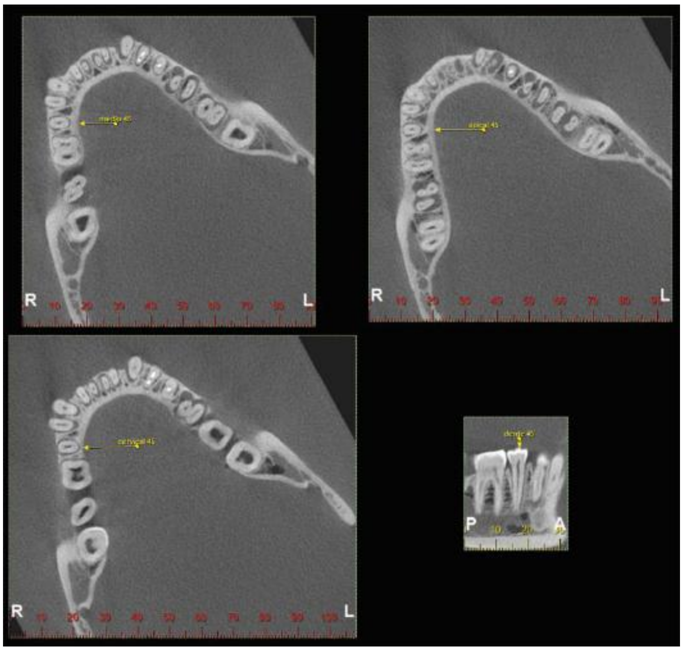

Source: Authors.

2.6 CNR assessment

For this phase of the study, premolars with their conduit endodontically treated and rehabilitated with an intracanal FP and resin cement or premolars that underwent endodontic treatment and post test (without resin cement) were selected. The participating groups were G1, G2, G3, and G4. Healthy premolars would not influence the production of artifacts and premolars with endodontic treatment were not part of the aim of the study. An objective analysis of the images was performed in the axial sections using the Image J software (National Institutes of Health, Bethesda, USA; http://rsb.info.nih.gov/ij/). On the axial plane, a circular region of interest (ROI) was selected in three areas of the root, i.e., apical, middle and cervical thirds (Figure 2).

Figure 2. Objective analysis aiming to obtain a histogram with the mean, minimum and maximum values of the region of interest (ROI) of the tooth (cervical third) using the Image J program and the registration spreadsheet.

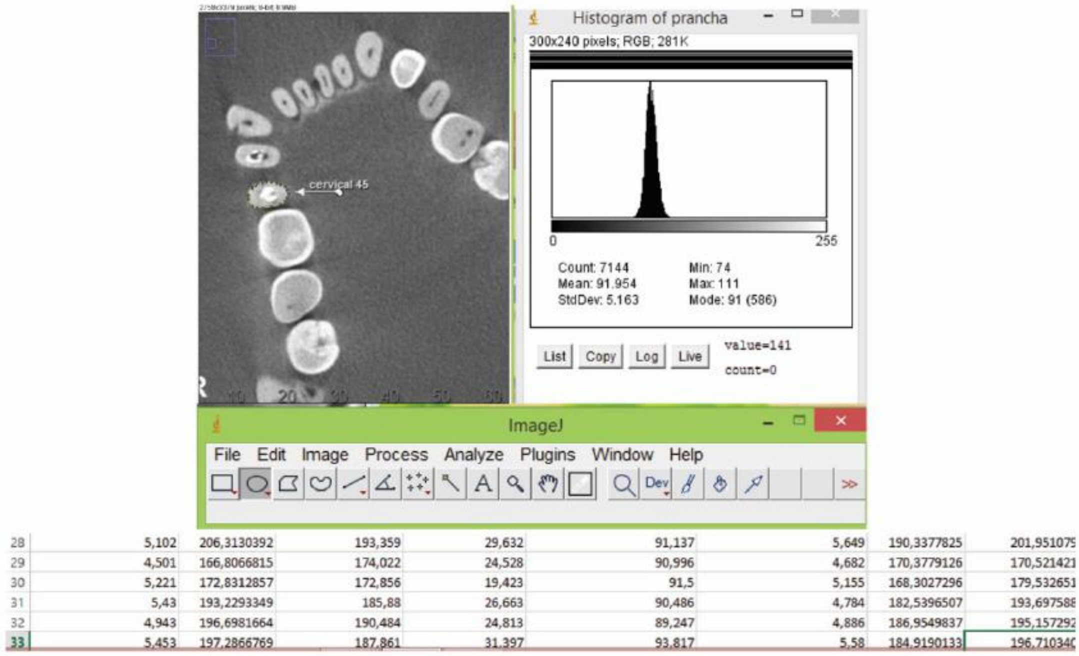

Source: Authors.

After calibration, the selection of the ROI was performed manually, encompassing the central region of the tooth structure and discarding the tissues surrounding the tooth, allowing an analysis of the site of artifact formation in the root region. For each ROI, the software provided a histogram with the standard deviation and the mean values of the gray tones present in the pixels. These values were recorded. Next, an arithmetic mean of the values of the three regions (cervical, middle and apical thirds) was obtained with a final value for each tooth, registered in a table and forming the database for statistics. Simultaneously, in order to obtain the CNR, a control area was also evaluated. A ROI was selected in the standardized lateral and outermost region of the acquired volume, with the same size used for evaluation in the region with artifact formation. Through the acquired values, the CNR was measured according to the following formula:

$$CNR = \frac{|Mean_{tooth} - Mean_{control}|}{\sqrt{SD_{tooth}^2 + SD_{control}^2}}$$

Where $Mean_{tooth}$ corresponds to the mean of the gray values of the ROI of the root, $Mean_{control}$ is the mean of the gray values of the ROI of the control area, and SD_{tooth} and $SD_{control}$, is the standard deviation of the root and control area, respectively (Fontenele *et al*, 2018). The difference between the minimum and maximum grayscale values provided by the histogram of the three root regions (apical, middle and cervical thirds) provides the variation in grayscale, resulting in a value for each tooth evaluated.

2.7 Data analysis

The Statistical Package for the Social Sciences (SPSS) software (IBM SPSS Statistics for Windows, version 25.0, Armonk, NY: IBM Corp.) was used for statistical analysis. Data were descriptively analyzed using measures of central tendency and measures of dispersion. To assess the difference between groups in terms of location variables (three thirds), the Kolmogorov-Smirnov test and the Shapiro-Wilk test were employed for quantitative variables according to the sample size. In the analysis of numerical variables, the ANOVA test for independent samples was employed in the comparison between groups and thirds. In the analysis of the location of thirds (within the length of the post – 2/3 thirds of the root) the Kruskal-Wallis test was employed to evaluate the presence or absence of artifacts. For all analyses, the level of significance was set at < 0.05.

3. Results

Table 1 summarizes the distribution of CNR results by group of teeth with materials present in the root canal (G1, G2, G3, and G4) regarding the location of the FP thirds (cervical, middle and apical). There was a statistically significant difference in the mean value of the middle third region regarding the groups analyzed (*p*=0.026). This result was between the Allcem Core group (G3) and post test of FP (G4). For the G3 group, no significant difference was observed in the cervical and apical thirds. In addition, Nexus 3 (G1) and Duo-Link (G2) resin cements and the G4 group had statistically similar means CNR values in all three thirds (i.e., cervical, middle and apical).

Table 1. Evaluation of contrast-noise ratio by group in relation to location thirds of teeth).

Variables	**Mean±SD**	***p* value***
Cervical third		
Nexus 3 (G1)	199.48±12.58	
Duolink (G2)	195.15±8.48	0.126
Allcem Core (G3)	198.51±9.88	
Post test (G4)	187.61±11.56	
Middle third		
Nexus 3 (G1)	197.14±8.65	
Duolink (G2)	190.61±9.26	**0.026**
Allcem Core (G3)	197.61±3.33	
Post test (G4)	184.28±12.60[A]	
Apical third		
Nexus 3 (G1)	188.62±3.05	
Duo-link (G2)	185.36±8.92	0.114
Allcem Core (G3)	191.54±5.28	
Post test (G4)	183.29±7.74	

Note: SD, standard deviation; *ANOVA test; [A]Statistically significant difference in relation to the “Allcem Core” group. Source: Authors

Table 2 depicts the distribution of the CNR results for all groups (G1, G2, G3, and G4) according to location in the thirds. Regardless of the material used, there was a statistically significant difference when comparing the thirds (*p*=0.010). This difference occurred between the cervical and apical location. When the analysis considered the groups as a whole, all of them showed artifacts with no statistically significant difference (*p*>0.05).

Table 2. Distribution of contrast-noise ratio results in root thirds of teeth in the studied groups.

	Location of thirds of teeth			
	Cervical	Middle	Apical	*p* value
Variables	**Mean±SD**	**Mean±SD**	**Mean±SD**	
All groups	194.53±11.02	191.63±10.43	186.88±7.47[A]	**0.010***
Nexus 3 (G2)	199.48±12.58	197.14±8.65	188.62±3.05	0.403**
Duo-link (G2)	195.15±8.48	190.61±9.26	185.36±8.92	0.086*
Allcem Core (G3)	198.51±9.88	197.61±3.33	191.54±5.28	0.104*
Post test (G4)	187.61±11.56	184.28±12.60	183.29±7.74	0.680*

SD, standard deviation; *ANOVA; **Kruskal-Wallis test; [A]Statistically significant difference regarding the cervical location of the tooth. Source: Authors.

4. Discussion

Premolar teeth are often more bulky than anterior teeth and generally uniradicular with relatively small pulp chambers. Thus, they often require the use of intracanal posts to restore function and esthetics (Carvalho *et al*, 2018). For these reasons, in the present study, this group of teeth was chosen to compose the experimental group and to more accurately simulate daily clinical situations. Furthermore, the use of FP in intracanal rehabilitations is growing in the literature and is a reality in dental clinics (Erik; Erik; Yıldırım, 2019). Their physical, chemical and biological interactions, in addition to the practicality of use, rationalize their choice as intraradicular retainers in this type of research.

Herein, we investigated the influence of different compositions of resin adhesive systems and, consequently, different degrees of radiopacity on the formation of artifacts. CNR is considered to be a standard factor for the evaluation of image quality, regardless of pixel size, compression, or output unit (Bayrak et al.,2020; Yang, 2016). It is known that the same material exhibits different CNR values at different exposure parameters (Bayrak et al.,2020). However, many noise reduction strategies have been proposed thus far and employed to improve the signal-to-noise ratio through CBCT slices in the image domain using different algorithms (Yang, 2016). The noise that corresponds to the calibrated projection data after logarithm transformation is signal dependent and the CNR objectively assesses the image quality, measuring the production of artifacts. Thus, it is possible to quantify the presence of the artifact and to compare the materials in a simplified way, making the methodology suitable for the proposal to be investigated. Accordingly, former studies have used CNR to assess the effects of algorithms on the quality of the images formed and its interpretation was based on a simple understanding (Bechara *et al*, 2012; Demirturk Kocasarac *et al*, 2016; Pauwels *et al*, 2013).

During sample analysis of the CNR among the thirds (cervical, middle and apical) of the FP, regarding the intracanal material present, the region of the middle third revealed a statistically significant difference between the Allcem Core (G3) and the post test (G4) groups. The G4 group, indeed, had a lower CNR and, consequently, a higher artifact; and only the FP test was able to interfere with the CNR. Nonetheless, the presence of an artifact when there is no cement interposed between the tooth structure and the root canal may result in little or no influence of the radiopacifiers of the studied resin cements on image quality. Yet, FP density was able to generate artifacts.

Previous studies have shown that, even when the resin adhesive system is not present, the quality of the CBCT image can be impaired, supporting the interpretation of images in which FP influence the production of artifacts (Diniz de Lima *et al*, 2019; Erik; Erik; Yıldırım, 2019). In fact, CBCT image artifacts can be attributed to multiple sources, including patient, digitizer, field of view, and nature of the X-ray beam projection (Vasconcelos *et al*, 2015), and therefore not just to the object to be analyzed. In endodontically treated teeth, for instance, the materials involved can interfere with radiopacity, reduce contrast and darken structures, compromising image quality, and interfering with interpretation (Bechara *et al*, 2013). In a former study, the images of the FP were similar to those of the group of teeth without intracanal restoration; however, the images of the artifacts obtained in that study were not quantified according to mean CNR value (Rabelo *et al*, 2017). Thus, image quantification by CNR provides a more reliable perception of the detection and measurement of artifacts.

In our study, different materials employed for cementation produced artifacts with similar CNR. However, in the study by Diniz de Lima *et al* (2019), FP with or without a metal core, produced fewer image artifacts in CBCT scans compared to metal posts and teeth endodontically treated only with intracanal obturator material, especially when associated with low exposure protocols. The authors supported the idea that FP could be an alternative to metal posts from a perspective of less artifact formation. The metallic artifact is produced because of the high density of the metal, making computer measurement difficult and degrading image quality (Panjnoush *et al*, 2016). Panjnoush *et al* (2016) reported that the type of metal, a chromium-cobalt alloy commonly used in metallic intraradicular retainers, had the greatest effect on the intensity of the artifact alloy. Nonetheless, considering clinical practicality, FP have better physicochemical properties and produce fewer artifacts compared to metallic posts (Diniz de Lima *et al*, 2019).

Notably, we observed that the middle third of FP in the G3 group (Allcem Core) had the highest CNR. Under normal conditions, the middle third is the location with a better condition for adaptation between the post and the adhesive agent to the dental substrate and for evaluating the CNR, favoring radiographic distinction between the tissues and restorative materials. CNR evaluation resulted in similar gray tones, i.e., with few variations between white and absolute black densities. The radiopacity property has a measurement limit, since, from a certain pixel value, the radiographic images will show practically the same shade of gray. Therefore, a quality image should have medium contrast and density in order to obtain sufficient information, avoiding diagnostic doubts and inadequate clinical procedures.

In addition to the relationship between the thirds of the FP, the amount of charge and consequent radiopacity may have influenced the production of artifacts. Of the studied resin cements, Nexus™, Duo-link, and Allcem Core have radiopacity in accordance with the ISO 4049/2009 standards (Walcher *et al*, 2019). The composition of Nexus™ contains ytterbium trifluoride. Allcem Core contains barium aluminum silicate glass microparticles and silicon dioxide nanoparticles used as filler, for a total of approximately 62% by weight, yet providing a weight increase in radiopacity (Walcher *et al*, 2019). In our study, the greater amount of charge contained in the Allcem Core formulation may have generated a positive factor in the CNR, confirming its better performance in the production of artifacts, specifically in the middle third, compared to the group with only the post test. On the other hand, according to Walcher *et al* (2019), the presence of an inorganic filler does not interfere with the evaluation of the physical and chemical properties of the bonding agent.

In the interpretation of CBCT images, resin adhesive agents had similar characteristics concerning the CNR, even with the use of artifices to improve the image. Along this line, in the search for better images, Rabelo *et al* (2017) and Diniz de Lima *et al* (2019) reported that CBCT acquisition protocols were modified in order to reduce the production of artifacts, including the use of enhancement filters. Ferreira *et al* (2015) when evaluating the influence of CBCT image enhancement filters on the diagnosis of fractures in teeth with and without metal posts, observed that the accuracy of images with and without a filter does not influence the diagnosis of fractures. Nonetheless, quantitative assessment of CBCT artifacts is usually performed on one or more slices, which can be a limitation. According to Rabelo *et al* (2017), the ideal would be for the assessment to incorporate the entire volume of the CBCT, as is done for the qualitative assessment. Likewise, isolating artifacts three-dimensionally has been a challenge. New segmentation software should be tested in order to isolate artifacts from the entire image volume, as well as the development of exposure protocols aimed at reducing artifacts.

5. Conclusion

In the CNR analysis, no difference was observed among the resin cements regarding the production of artifacts. It is important to emphasize that artifacts were produced regardless of the resin cement used, or even without the presence of cement interposed between the FP and the tooth structure. Thus, the choice of resin cements should preferably be based on ease of handling, working time, cost-effectiveness, activation modes, and clinical aspects. Further studies evaluating lower exposure protocols associated with image quality and the formation of artifacts are still needed.

Acknowledgments

The authors thank the Coordination for the Improvement of Higher Education Personnel (CAPES, Finance Code 001). Mrs. E. Greene provided English editing of the manuscript.

References

Altintas, S. H., Yildirim, T., Kayipmaz, S., & Usumez, A. (2013). Evaluation of the radiopacity of luting cements by digital radiography. *Journal of Prosthodontics*, 22(4), 282–286.

Antonijevic, D., Jevremovic, D., Jovanovic, S., & Obradovic-Djuricic, K. (2012). An in vitro radiographic analysis of the density of dental luting cements as measured by CCD-based digital radiography. *Quintessence International*, 43(5), 421–428.

Bayrak, S., Kursun Cakmak, E. S., & Kamalak, H. (2020). Contrast-to-noise ratios of different dental restorative materials: an in-vitro cone beam computed tomography study. *European Oral Research*, 54(1), 36–41.

Bechara, B. B., Moore, W. S., McMahan, C. A., & Noujeim, M. (2012). Metal artefact reduction with cone beam CT: an in vitro study. *Dento Maxillo Facial Radiology*, 41(3), 248–253.

Bechara, B., Alex McMahan, C., Moore, W. S., Noujeim, M., Teixeira, F. B., & Geha, H. (2013). Cone beam CT scans with and without artefact reduction in root fracture detection of endodontically treated teeth. *Dento Maxillo Facial Radiology*, 42(5), 20120245.

Carvalho, M. A., Lazari, P. C., Gresnigt, M., Del Bel Cury, A. A., & Magne, P. (2018). Current options concerning the endodontically-treated teeth restoration with the adhesive approach. *Brazilian Oral Research*, 32(suppl 1), e74.

Carvalho, R.L.S. de., Spinelli, F. de L.C., Mendonça, L.S. de., Arruda, J.A.A. de., Moreno, A., Alvares, P.R., Rodrigues, C.D., Sobral, A.P.V., & Silveira, M.M.F. da. (2021). Detection of vertical root fractures in the presence of artefacts by digital radiography and cone beam computed tomography. *Research, Society and Development*, 10, e284101018393.

Celikten, B., Jacobs, R., deFaria Vasconcelos, K., Huang, Y., Nicolielo, L., & Orhan, K. (2017). Assessment of volumetric distortion artifact in filled root canals using different cone-beam computed tomographic devices. *Journal of Endodontics*, 43(9), 1517–1521.

Demirturk Kocasarac, H., Helvacioglu Yigit, D., Bechara, B., Sinanoglu, A., & Noujeim, M. (2016). Contrast-to-noise ratio with different settings in a CBCT machine in presence of different root-end filling materials: an in vitro study. *Dento Maxillo Facial Radiology*, 45(5), 20160012.

Diniz de Lima, E., Lira de Farias Freitas, A. P., Mariz Suassuna, F. C., Sousa Melo, S. L., Bento, P. M., & Pita de Melo, D. (2019). Assessment of cone-beam computed tomographic artifacts from different intracanal materials on birooted teeth. *Journal of Endodontics*, 45(2), 209–213.e2.

Draenert, F. G., Coppenrath, E., Herzog, P., Müller, S., & Mueller-Lisse, U. G. (2007). Beam hardening artefacts occur in dental implant scans with the NewTom cone beam CT but not with the dental 4-row multidetector CT. *Dento Maxillo Facial Radiology*, 36(4), 198–203.

Dukic W. (2019). Radiopacity of composite luting cements using a digital technique. *Journal of Prosthodontics*, 28(2), e450–e459.

Erik, A. A., Erik, C. E., & Yıldırım, D. (2019). Experimental study of influence of composition on radiopacity of fiber post materials. *Microscopy Research and Technique*, 82(9), 1448–1454.

Estrela, C., Pécora, J. D., Souza-Neto, M. D., Estrela, C. R., & Bammann, L. L. (1999). Effect of vehicle on antimicrobial properties of calcium hydroxide pastes. *Brazilian Dental Journal*, 10(2), 63–72.

Fagundes, D., de Mendonça, I. L., de Albuquerque, M. T., & Inojosa, I. (2014). Spontaneous healing responses detected by cone-beam computed tomography of horizontal root fractures: a report of two cases. *Dental Traumatology*, 30(6), 484–487.

Ferreira, L. M., Visconti, M. A., Nascimento, H. A., Dallemolle, R. R., Ambrosano, G. M., & Freitas, D. Q. (2015). Influence of CBCT enhancement filters on diagnosis of vertical root fractures: a simulation study in endodontically treated teeth with and without intracanal posts. *Dento Maxillo Facial Radiology*, 44(5), 20140352.

Fonseca, R. B., Branco, C. A., Soares, P. V., Correr-Sobrinho, L., Haiter-Neto, F., Fernandes-Neto, A. J., & Soares, C. J. (2006). Radiodensity of base, liner and luting dental materials. *Clinical Oral Investigations*, 10(2), 114–118.

Fontenele, R. C., Nascimento, E. H., Vasconcelos, T. V., Noujeim, M., & Freitas, D. Q. (2018). Magnitude of cone beam CT image artifacts related to zirconium and titanium implants: impact on image quality. *Dento Maxillo Facial Radiology*, 47(6), 20180021.

Freitas, D. Q., Fontenele, R. C., Nascimento, E., Vasconcelos, T. V., & Noujeim, M. (2018). Influence of acquisition parameters on the magnitude of cone beam computed tomography artifacts. *Dento Maxillo Facial Radiology*, 47(8), 20180151.

Furtos, G., Baldea, B., Silaghi-Dumitrescu, L., Moldovan, M., Prejmerean, C., & Nica, L. (2012). Influence of inorganic filler content on the radiopacity of dental resin cements. *Dental Materials Journal*, 31(2), 266–272.

Goracci, C., Juloski, J., Schiavetti, R., Mainieri, P., Giovannetti, A., Vichi, A., & Ferrari, M. (2015). The influence of cement filler load on the radiopacity of various fibre posts ex vivo. *International Endodontic Journal*, 48(1), 60–67.

Krithikadatta, J., Gopikrishna, V., & Datta, M. (2014). CRIS Guidelines (Checklist for Reporting In-vitro Studies): A concept note on the need for standardized guidelines for improving quality and transparency in reporting in-vitro studies in experimental dental research. *Journal of Conservative Dentistry*, 17(4), 301–304. https://doi.org/10.4103/0972-0707.136338

Lin, H. H., Chiang, W. C., Lo, L. J., Sheng-Pin Hsu, S., Wang, C. H., & Wan, S. Y. (2013). Artifact-resistant superimposition of digital dental models and cone-beam computed tomography images. *Journal of Oral and Maxillofacial Surgery*, 71(11), 1933–1947.

Nascimento, E., Fontenele, R. C., Santaella, G. M., & Freitas, D. Q. (2019). Difference in the artefacts production and the performance of the metal artefact reduction (MAR) tool between the buccal and lingual cortical plates adjacent to zirconium dental implant. *Dento Maxillo Facial Radiology*, 48(8), 20190058.

Panjnoush, M., Kheirandish, Y., Kashani, P. M., Fakhar, H. B., Younesi, F., & Mallahi, M. (2016). Effect of Exposure Parameters on Metal Artifacts in Cone Beam Computed Tomography. *Journal of Dentistry*, 13(3), 143–150.

Pauwels, R., Stamatakis, H., Bosmans, H., Bogaerts, R., Jacobs, R., Horner, K., Tsiklakis, K., & SEDENTEXCT Project Consortium (2013). Quantification of metal artifacts on cone beam computed tomography images. *Clinical Oral Implants Research*, 24 Suppl A100, 94–99.

Pedrosa, R. F., Brasileiro, I. V., dos Anjos Pontual, M. L., dos Anjos Pontual, A., & da Silveira, M. M. (2011). Influence of materials radiopacity in the radiographic diagnosis of secondary caries: evaluation in film and two digital systems. *Dento Maxillo Facial Radiology*, 40(6), 344–350.

Petersson, A., Axelsson, S., Davidson, T., Frisk, F., Hakeberg, M., Kvist, T., Norlund, A., Mejàre, I., Portenier, I., Sandberg, H., Tranaeus, S., & Bergenholtz, G. (2012). Radiological diagnosis of periapical bone tissue lesions in endodontics: a systematic review. *International Endodontic Journal*, 45(9), 783–801.

Rabelo, K. A., Cavalcanti, Y. W., de Oliveira Pinto, M. G., Sousa Melo, S. L., Campos, P., de Andrade Freitas Oliveira, L. S., & de Melo, D. P. (2017). Quantitative assessment of image artifacts from root filling materials on CBCT scans made using several exposure parameters. *Imaging Science in Dentistry*, 47(3), 189–197.

Rodriguez-Molares, A., Rindal, O., D'hooge, J., Masoy, S. E., Austeng, A., Lediju Bell, M. A., & Torp, H. (2020). The generalized contrast-to-noise ratio: a formal definition for lesion detectability. *IEEE Transactions on Ultrasonics, Ferroelectrics, and Frequency Control*, 67(4), 745–759.

Rubo, M. H., & el-Mowafy, O. (1998). Radiopacity of dual-cured and chemical-cured resin-based cements. *The International Journal of Prosthodontics*, 11(1), 70–74.

Schulze, R., Heil, U., Gross, D., Bruellmann, D. D., Dranischnikow, E., Schwanecke, U., & Schoemer, E. (2011). Artefacts in CBCT: a review. *Dento Maxillo Facial Radiology*, 40(5), 265–273.

Soares, C. J., Rodrigues, M. P., Faria-E-Silva, A. L., Santos-Filho, P., Veríssimo, C., Kim, H. C., & Versluis, A. (2018). How biomechanics can affect the endodontic treated teeth and their restorative procedures? *Brazilian Oral Research*, 32(suppl 1), e76.

Takeshita, W. M., Santos, L. R. A., Castilho, J. C. M., Médici Filho, E. M., Moraes, L. C., Sannomiya, E. K. (2004). An investigation of the optical density of composite resin using digital radiography. *Ciência Odontológica Brasileira*, 7(2), 6–11.

Tanomaru-Filho, M., da Silva, G. F., Duarte, M. A., Gonçalves, M., & Tanomaru, J. M. (2008). Radiopacity evaluation of root-end filling materials by digitization of images. *Journal of Applied Oral Science*, 16(6), 376–379.

Toyooka, H., Taira, M., Wakasa, K., Yamaki, M., Fujita, M., & Wada, T. (1993). Radiopacity of 12 visible-light-cured dental composite resins. *Journal of Oral Rehabilitation*, 20(6), 615–622.

van Dijken, J. W., Wing, K. R., & Ruyter, I. E. (1989). An evaluation of the radiopacity of composite restorative materials used in Class I and Class II cavities. *Acta Odontologica Scandinavica*, 47(6), 401–407.

Vasconcelos, K. F., Nicolielo, L. F., Nascimento, M. C., Haiter-Neto, F., Bóscolo, F. N., Van Dessel, J., EzEldeen, M., Lambrichts, I., & Jacobs, R. (2015). Artefact expression associated with several cone-beam computed tomographic machines when imaging root filled teeth. *International Endodontic Journal*, 48(10), 994–1000.

Walcher, J. G., Leitune, V., Collares, F. M., de Souza Balbinot, G., & Samuel, S. (2019). Physical and mechanical properties of dual functional cements-an in vitro study. *Clinical Oral Investigations*, 23(4), 1715–1721.

Yang C. C. (2016). Characterization of scattered X-ray photons in dental cone-beam computed tomography. *PloS one*, 11(3), e0149904.